IUBMB *Life*, 61(12): 1143–1152, December 2009

Research Communication

Enzymatic Processing of β-Dystroglycan Recombinant Ectodomain By MMP-9: Identification of the Main Cleavage Site

Manuela Bozzi[1*], Rosanna Inzitari[1*], Diego Sbardell[2], Susanna Monaco[2], Ernesto Pavoni[1], Magda Gioia[2], Stefano Marini[2], Simona Morlacchi[3], Francesca Sciandra[4], Massimo Castagnola[1], Bruno Giardina[1], Andrea Brancaccio[4] and Massimo Coletta[2]

[1]*Istituto di Biochimica e Biochimica Clinica, Università Cattolica del Sacro Cuore, Roma, Italy*
[2]*Dipartimento di Medicina Sperimentale e Scienze Biochimiche, Università di Roma Tor Vergata, Roma, Italy*
[3]*Dipartimento di Biologia Animale ed Ecologia Marina, Università degli Studi di Messina, Italy*
[4]*Istituto di Chimica del Riconoscimento Molecolare (CNR), Sezione di Roma, Roma, Italy*

Summary

Dystroglycan (DG) is a membrane receptor belonging to the complex of glycoproteins associated to dystrophin. DG is formed by two subunits, α-DG, a highly glycosylated extracellular matrix protein, and β-DG, a transmembrane protein. The two DG subunits interact through the C-terminal domain of α-DG and the N-terminal extracellular domain of β-DG in a non-covalent way. Such interaction is crucial to maintain the integrity of the plasma membrane. In some pathological conditions, the interaction between the two DG subunits may be disrupted by the proteolytic activity of gelatinases (i.e. MMP-9 and/or MMP-2) that removes a portion or the whole β-DG ectodomain producing a 30 kDa truncated form of β-DG. However, the molecular mechanism underlying this event is still unknown. In this study, we carried out proteolysis of the recombinant extracellular domain of β-DG, β-DG(654-750) with human MMP-9, characterizing the catalytic parameters of its cleavage. Furthermore, using a combined approach based on SDS-PAGE, MALDI-TOF and HPLC-ESI-IT mass spectrometry, we were able to identify one main MMP-9 cleavage site that is localized between the amino acids His-715 and Leu-716 of β-DG, and we analysed the proteolytic fragments of β-DG(654-750) produced by MMP-9 enzymatic activity.
IUBMB *Life*, 61: 1143–1152, 2009

Keywords dystroglycan; MMP-9; mass spectrometry.

Abbreviations DG, dystroglycan; MMP, matrix metalloproteinase; MALDI TOF-MS, matrix-assisted laser desorption ionization time-of-flight mass spectrometry; ESI, electrospray ionization; RP-HPLC, reverse-phase high-performance liquid chromatography; SDS-PAGE, sodium dodecyl sulphate polyacrylamide gel electrophoresis; TIC, total ion current; XIC, extracted ion current.

INTRODUCTION

Dystroglycan (DG) is a widely expressed heterodimeric glycoprotein consisting of an extracellular subunit, α-DG of 120–200 kDa, and a transmembrane subunit, β-DG of 43 kDa (*1*). α-DG interacts with other extracellular proteins, including laminin, perlecan and agrin (*2*), whereas β-DG is connected with cytosolic proteins, such as dystrophin, utrophin, rapsyn, caveolin-3 and Grb2 (*3–5*). The two DG subunits are associated in a non-covalent fashion through the C-terminal domain of α-DG and the N-terminal extracellular domain of β-DG (*6*), ensuring a contact between the extracellular matrix and the cytoskeleton. The interactions that DG subunits establish with extracellular and intracellular partners are significantly altered in distinct congenital or late-onset muscular dystrophies, characterized by muscular weakness, necrosis and mental retardation (*7, 8*). This is observed, for example, as a consequence of the α-DG

Received 20 July 2009; accepted 22 September 2009
*These two authors have equally contributed to this work.
Unità NeuroGlia, DIBIT, Istituto Scientifico San Raffaele, Milano, Italy

Address correspondence to: Massimo Coletta, Dipartimento di Medicina Sperimentale e Scienze Biochimiche, Università di Roma Tor Vergata, Via Montpellier 1, I-00133 Roma, Italy. E-mail: coletta@seneca.uniroma2.it or Andrea Brancaccio, Istituto di Chimica del Riconoscimento Molecolare (CNR), c/o Istituto di Biochimica e Biochimica Clinica, Università Cattolica del Sacro Cuore, Largo Francesco Vito, 1- 00168 Roma, Italy. E-mail: andrea.brancaccio@icrm.cnr.it.

ISSN 1521-6543 print/ISSN 1521-6551 online
DOI: 10.1002/iub.273

hypoglycosylation due to aberrations of the genes encoding for some glycosyltransferases (such as LARGE, POMT1, POMT2 and others), which impairs the interaction between α-DG and other extracellular proteins, especially laminin (*8*). Furthermore, disruption of the α-DG/β-DG interface is associated as well with dramatic effects, such as sarcolemma instability followed by muscular necrosis. This cascade of events indeed is occurring in the presence of defects of the dystrophin gene associated to the Duchenne muscular dystrophy, where the loss of the α-DG/β-DG interaction can be frequently observed within the skeletal muscle of patients affected by such disease (*7*).

Disruption of the α-DG/β-DG interface was also observed in specific breast cancer cell lines, where a 30 kDa truncated form of β-DG, produced by the shedding of its extracellular domain, was reported (*9*). Further studies suggested that some metalloproteinases could be responsible for the production of the 30 kDa β-DG truncated form which was also detected, although in reduced amounts, in healthy tissues, such as peripheral nerve, bladder, lung, kidney (*10*) and in normal human keratinocytes (*11*). The presence of the 30 kDa β-DG fragment has been reported under different pathological conditions of the skeletal muscle, such as Duchenne muscular dystrophy, Fukuyama-type congenital dystrophy and sarcoglycanopathy (*12*). The 30 kDa β-DG fragment was also detected in tissues subjected to ischemic injury (*13, 14*) and in joint tissues from patients affected by osteoarthritis (*15*); finally, β-DG degradation was also discovered in some forms of epithelial cancerous cells (*16*). In any case, the 30 kDa β-DG fragment lacks all or part of the β-DG ectodomain, as it can be detected using the monoclonal antibody 43DAG directed against the C-terminus of β-DG.

Recently, the specific metalloproteinase activity on β-DG has been referred mostly to gelatinases (i.e., MMP-2 and MMP-9) (*17, 18*), a class of matrix metalloproteinases uniquely characterized by the presence of a fibronectin-like subdomain within the catalytic domain (*19, 20*), which is very important for substrate recognition (*21*) and activity modulation (*22*). Interestingly, β-DG has been proposed to be the first substrate digested by MMP-9 in response to enhanced neuronal activity, playing a role in synaptic plasticity, learning and memory (*23, 24*). These data suggest that modulating the α-DG/β-DG interaction may have a precise functional role and that MMP-9 may be involved in this physiological process.

Although the important role of the MMP-9 activity on β-DG functions is definitely assessed, the molecular mechanism underlying the β-DG cleavage remains still elusive (*25*). The purpose of this investigation is to characterise the enzymatic activity of human MMP-9 on the recombinant β-DG ectodomain, spanning the amino-acidic positions between residues 654 and 750, to identify possible cleavage site(s).

MATERIALS AND METHODS

Preparation of the Recombinant Proteins

All the DNA manipulations, required for the production of the recombinant N-terminal extracellular domain of β-DG, β-DG(654–750) and the C-terminal domain of α-DG, α-DG(485–630), have been already described elsewhere (*6*). Murine β-DG(654–750) and α-DG(485–630) recombinant fragments were expressed in E. coli BL21(DE3) as thioredoxin (Trx) fusion proteins that also contain a N-terminal His6-tag and a thrombin cleavage site (*26*). Bacterial cells were cultured at 37 °C in 1.2 L of normal LB medium to an OD at 600 nm of 0.8; cells were induced with IPTG and harvested after 3 hr. The cellular pellets were suspended in a lysis buffer containing 5 mM imidazole, 0.5 M NaCl, 20 mM Tris-HCl and 1 mM PMSF at pH 7.9. Cell lysis was achieved by sonication. The fusion proteins were purified using nickel nitrilotriacetate affinity chromatography. β-DG(654–750), with two foreign residues Gly-Ser at the N-term, and α-DG(485–630), with five foreign residues Gly-Ser-Arg-Val-Asp at the N-term, were obtained upon thrombin cleavage. The yield of the recombinant proteins was approximately 5 mg/L of bacterial culture.

Recombinant human full length MMP-9 was produced in Sf9 insect cells after transfection with a baculovirus carrying the MMP-9 cDNA (*27*). The secreted proMMP-9 was purified to homogeneity by gelatin-Sepharose chromatography (*28*) and dialyzed against 100 mM Tris/HCl pH 7.4, 100 mM NaCl, 10 mM $CaCl_2$. The proenzyme was activated by incubating a 10 μM progelatinase solution with a solution containing 0.1 μM of the catalytic domain of MMP-3 (Biomol International, USA) at 37 °C for 90 min. Recombinant human full length MMP-2 (R&D System) was obtained as a proteolytically active enzyme, thus not requiring any chemical or enzymatic activation.

Fragmentation Kinetics and Data Analysis

Kinetics of recombinant β-DG(654–750) ectodomain cleavage induced by MMP-9 have been carried out at 37 °C and pH 7.3, incubating different concentrations of substrate (spanning between 7 μM and 15 μM) in 50 mM Tris-HCl, 0.1 M NaCl and 10 mM $CaCl_2$, with 100 nM recombinant MMP-9. Aliquots of the reaction mixture were harvested at increasing incubation times, samples were run on a 12% polyacrylamide Tricine gel and stained with Coomassie brilliant blue. Substrate degradation (or fragment formation) velocity was determined analysing the spot density by laser scanning (LKB 2202 UltraScan). Catalytic parameters have been determined by double-reciprocal plots of velocity versus substrate concentration, according to the following equation:

$$\frac{[E_0]}{v} = \frac{K_m}{k_{cat} \times [S]} + \frac{1}{k_{cat}} \quad (1)$$

where $[E_0]$ is the total enzyme concentration, v is the velocity (expressed as mol/sec), K_m is the Michaelis-Menten constant, k_{cat} is the catalytic constant and $[S]$ is the substrate concentration. The applicability of this mechanism is checked by the linearity of experimental data on this double-reciprocal plot. To get a comparison with MMP-9, kinetics of recombinant β-DG(654–750) ectodomain cleavage induced by MMP-2 were performed under the same experimental conditions.

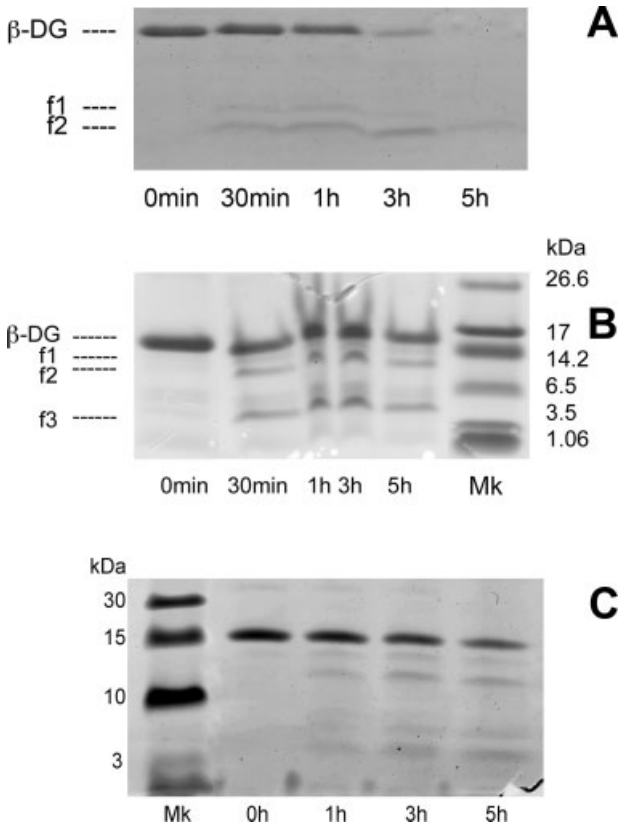

Figure 1. The proteolytic fragments of 20 μM β-DG(654–750), obtained upon incubation with 100 nM MMP-9 at 37°C, pH 7.3 for increasing times, were separated by 12% polyacrylamide SDS-PAGE Tricine gels run for 150 (A) and 90 min (B). A proteolytic digestion of β-DG(654–750) was also performed with MMP-2 under the same experimental conditions (C). The gels were treated with glutaraldehyde before staining with Coomassie brilliant blue.

In-Gel Trypsin Digestion and Extraction of Tryptic Peptides

Upon Coomassie staining, the bands of interest were excised from SDS polyacrylamide gels and treated with 10 mM DTT for 50 min and with 55 mM IAA for further 30 min. After a drying step with acetonitrile, the gel particles were rehydrated with 50 μl of digestion buffer (50 mM NH_4HCO_3 at pH 8) containing 12.5 ng/μl of pancreas bovine trypsin (Sigma St. Louis) and incubated at 4 °C for 45 min. Finally, the solution containing the gel particles was incubated overnight at 37 °C under mild mixing. The solution was then centrifuged at 4,000*g* for 3 min and the supernatant was collected. The gel pellet was washed with 1% TFA and with acetonitrile:0.1% TFA (1:1) and the supernatant was collected again. The final solution was concentrated in a vacuum centrifuge and suspended in 0.1% TFA. The digested peptides were premixed 1:1 with matrix solution (5g/L cyano-4-hydroxycinnamic acid (CHCA) in 50% ACN/0,1%TFA), deposited onto the stainless-steel target according to the dried droplet method (*29*) and analysed by MALDI-TOF MS (Bruker Daltonics, Bremen, Germany).

MALDI-TOF Spectra Collection

MALDI-TOF was used to obtain the peptide mass fingerprinting (PMF) data for each sample extracted from the polyacrylamide gel previously sliced. The analysis was performed on an Autoflex® Bruker Daltonics mass spectrometer (Bremen, Germany). MALDI-TOF mass spectra were acquired with a pulsed nitrogen laser (337 nm) in reflector mode. In positive reflector mode, spectra were obtained with an ion source of 19 kV, a pulsed ion extraction time of 150 ns, a detector gain voltage of 1,400V and a laser frequency of 5 Hz. The final mass spectra were produced by averaging 500 laser shots to improve signal-to-noise ratio. Calibration was performed using reference peptides (Angiotensin I and II, substance P and Bombesin). The mass spectra were processed with the Bruker's data-processing software (Flex Analysis) to obtain accurate average mass values. The MALDI-TOF peptide mass fingerprinting (PMF) data obtained were compared with the ones obtained from the SWISS-PROT database screening using PeptideMass (*30, 31*).

RP-HPLC ESI-MS and MS/MS Analysis

The HPLC-ESI MS apparatus was a ThermoFisher (San Jose, CA) Surveyor HPLC connected by a Tsplitter to a photodiode array detector and to a Xcalibur LCQ Deca XP Plus mass spectrometer. The mass spectrometer was equipped with an electrospray ion source. The chromatographic column was a Vydac (Hesperia, CA) C8 column, with 5 mm particle diameter (column dimensions 150 × 2.1 mm). The following solutions were utilized for the reversed-phase chromatography: (eluent A) 0.056% aqueous TFA and (eluent B) 0.050% TFA in acetonitrile: water 80:20 v/v. The gradient applied was linear from 0–55% of B in 40 min, at a flow-rate of 0.30 mL/min. The T splitter addressed a flow-rate of about 0.20 mL/min towards the diode array detector and a flow-rate of about 0.10 mL/min towards the ESI source. The diode array detector was set in the range 214–276 nm. Mass spectra were collected every 3 min in the positive ion mode. MS spray voltage was 4.50 kV and the capillary temperature was 220 °C. MS/MS experiments were performed by detecting the parent ions with a peak width of 2–4 m/z values and by using 40% of the maximum activation amplitude. Average ESI mass spectra deconvolution was automatically performed with the software provided by Deca-XP instrument (Bioworks Browser) or MagTran 1.0 software (*32*). Experimental mass values were compared with the average theoretical mass values using a PeptideMass program available at the Swiss-Prot (http://us.expasy.org/tools) data bank. The relative abundances of β-DG(654–750), and derivatives were approximately calculated by performing a multiple extracted ion current (XIC) search for every species. The XIC procedure is based on the extraction of the current associated to either one (single XIC) or more (multiple XIC) ions with selected m/z val-

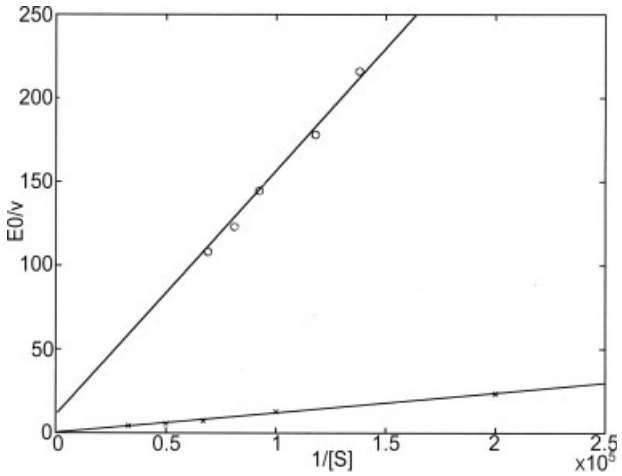

Figure 2. Double-reciprocal Lineweaver-Burk plot of β-DG(654–750) proteolytic cleavage induced by MMP-9 (o) and MMP-2 (x). Each continuous line is obtained by fitting experimental data to Eq. (1) (see Materials and Methods).

ues from the total ion current (TIC) profile. The most relevant m/z values were chosen to have a rough value of the total ion current connected to each protein/peptide. Under the constant analytical conditions applied in this study, it was possible to use the integrated ion current peak area for a rough estimation of relative peptide/protein abundances (*33, 34*).

RESULTS

Recombinant β-DG(654–750) spanning the N-terminal extracellular domain of β-DG is characterized by an anomalous electrophoretic mobility of the ~10.5 kDa peptide β-DG(654–750) (which has a M_r of approximately 14 kDa, Fig. 1); this is a physicochemical property shared with other proteins belonging to the class of the natively unfolded proteins (*35, 36*). Fig. 1A shows the β-DG(654–750) fragmentation pattern obtained by incubation with activated MMP-9 at pH 7.3 and 37 °C; the 14 kDa band corresponding to β-DG(654–750) progressively reduced its intensity, whereas two bands, f1 and f2, at around 7 kDa appeared after 30 min. To reveal possible low molecular mass products, a 12% polyacrylamide Tricine gel was run for shorter times and treated with glutaraldehyde before Coomassie brilliant blue staining, a procedure required to prevent the low molecular mass polypeptides from diffusing out of the gel. In Fig. 1B a band of about 3.5 kDa (f3) was well detectable after 30 min of incubation. The double band (f1 and f2) detected in Fig. 1A was not well resolved but could still be clearly detected.

To study the kinetics of β-DG(654–750) proteolysis, increasing concentrations of β-DG(654–750) were incubated with a fixed concentration of MMP-9 (100 nM), and depletion of the intact β-DG(654–750) band, running at 14 kDa in the Tricine gel, was measured by densitometry. The β-DG(654–750) consumption rate increased linearly between 7 μM and 15 μM; this suggested that β-DG(654–750) processing follows the Michaelis-Menten mechanism (see Fig. 2), and the catalytic parameters associated to the proteolytic event were calculated accordingly.

The enzymatic activity appeared to be fairly slow (as from a $k_{cat}/K_m = 6.8(\pm 0.8) \times 10^2\ M^{-1}\ s^{-1}$), a feature that must be attributed to a very slow rate-limiting step ($k_{cat} = 0.09(\pm 0.01)\ s^{-1}$), in spite of a relatively high affinity for the substrate (as from $K_m = 1.4(\pm 0.2) \times 10^{-4}$ M). This behaviour suggested that MMP-9 recognized quite efficiently β-DG(654–750), but the enzyme:substrate complex displayed some steric impairment for the enzymatic cleavage event, thus raising its activation free energy barrier. This feature can find an explanation in the partially unfolded structure of the β-DG ectodomain (*37, 38*), that after the formation of the enzyme:substrate complex is likely to undergo a sort of conformational rearrangement for the enzyme catalytic site to come into contact with the cleavage site(s).

Since MMP-2 also targets β-DG *in vivo* (*17–19*), its enzymatic activity has been tested on the recombinant β-DG (654–750) and compared with the one displayed by MMP-9. MMP-2 produced four proteolytic fragments (see Fig. 1C) following a Michaelis-Menten mechanism (see Fig.2). Comparing the catalytic parameters featuring the proteolytic cleavage of β-DG (654–750), it can be deduced that MMP-2 and MMP-9 display the same affinity for β-DG(654–750) ($K_m = 4.5(\pm 0.6) \times 10^{-4}$M for MMP-2 and $K_m = 1.4(\pm 0.2) \times 10^{-4}$ M for MMP-9), but MMP-2 exhibits a higher enzymatic activity ($k_{cat}/K_m = 8.5(\pm 1.3) \times 10^3\ M^{-1}s^{-1}$, $k_{cat} = 3.85(\pm 0.53)\ s^{-1}$ for MMP-2 and $k_{cat}/K_m = 6.8(\pm 0.8) \times 10^2\ M^{-1}s^{-1}$, $k_{cat} = 0.09(\pm 0.01)\ s^{-1}$ for MMP-9).

To identify the β-DG(654–750) proteolytic fragments produced by MMP-9, a MALDI-TOF MS analysis was carried out on the electrophoretic bands showed in Figs. 1A and 1B. After in-gel tryptic digestion of the excised bands and extraction of the products (see Materials and Methods for details), the peptides were analysed by MALDI-TOF MS. The experimental m/z values obtained from the spectrum of the full-length β-DG(654–750) have been compared with the theoretical values calculated using the PeptideMass software (www.expasy.org) (*30, 31*). Data analysis has been addressed only to the experimental m/z values which satisfied the following requirements: (i) a signal-to-noise ratio higher than 10, (ii) a difference between theoretical and averaged measured mass $\leq$ 1Da.

The MALDI-TOF MS spectra obtained by tryptic digestion of the three bands detected on the Tricine gel reported in Fig. 1A allowed the identification of eight peptides covering 100% of the β-DG(654–750) primary sequence of the full-length β-DG 14 kDa band (see Table 1). In the case of the f1 band, three peptides have been assigned spanning the following amino acid positions: (i) from 672 to 679, (ii) from 680 to 701, (iii) from 681 to 701 (see Table 1). For the f2 band, three peptides have been detected and identified within the following amino acid positions: (i) 654– 671 (in addition to the two foreigner residues GS at the N-terminus), (ii) 672–679, and (iii) 681–701 (see Table 1). The spectrum obtained by tryptic digestion of the

Table 1

MALDI-TOF MS analysis of the proteolytic peptides obtained by tryptic digestion of the three bands detected on the Tricine gel reported in Fig. 1A, corresponding to non-reacted full-length β-DG(654-750) and its fragments f1 and f2

Position	Measured mass (Da) $[M+H]^+$avg	Theoretical mass (Da) $[M+H]^+$avg	Delta mass(Da)	Missed cleavage Sites	Sequence
			Nonreacted full-length β-DG(654–750)		
GS-654–671	2241.183	2241.122	−0.061	0	GSSIVVEWTNNTLPLEPCPK
672–679	915.568	915.526	−0.042	0	EQIIGLSR
680–701	2472.350	2472.263	−0.087	1	R IADENGKPRPAFSNALEPDFK
681–701	2316.245	2316.162	−0.083	0	IADENGKPRPAFSNALEPDFK
702–714	1278.706	1278.647	−0.058	0	ALSIAVTGSGSCR
715–739	2541.455	2541.310	−0.145	0	HLQFIPVAPPSPGSSAAPATEVPDR
715–743	3010.730	3010.527	−0.203	1	HLQFIPVAPPSPGSSAAPATEVPDRDPEK
715–750	3806.105	3805.819	−0.285	2	HLQFIPVAPPSPGSSAAPATEVPDRDPEKSSEDDVY
			f1 band		
672–679	915.425	915.526	0.100	0	EQIIGLSR
680–701	2471.965	2472.263	0.297	1	R IADENGKPRPAFSNALEPDFK
681–701	2316.063	2316.162	0.098	0	IADENGKPRPAFSNALEPDFK
			f2 band		
GS-654–671	2241.112	2241.122	0.009	0	GSSIVVEWTNNTLPLEPCPK
672–679	915.544	915.526	−0.018	0	EQIIGLSR
681–701	2317.166	2316.162	−1.004	0	IADENGKPRPAFSNALEPDFK
			f3 band		
716–739	2404.257	2404.251	−0.006	1	LQFIPVAPPSPGSSAAPATEVPDR

For each peptide are reported: the amino acidic positions within the β-DG primary structure (first column), the measured (second column) and calculated mass values (third column), the difference between the theoretical and measured mass values (forth column), the missed cleavages (fifth column), and the amino acid sequences (sixth column).

f3 band at around 3.5 kDa, reported in the gel of Fig. 1B, detected a single peptide covering the amino acid positions comprised between 716 and 739 of β-DG(654–750). These data indicated that MMP-9 degraded β-DG(654–750) producing three proteolytic fragments, corresponding to the f1, f2 and f3 bands, f1 and f2 shared at least two tryptic fragments spanning the amino acid positions 672–679 and 681–701 of β-DG, whereas f3 seemed to belong to the C-terminal portion of β-DG as it contained a proteolytic fragment spanning the amino acid positions 716–739. Based on this evidence, although the low amount of peptide contained in each band prevented the detection of all the tryptic fragments expected, we could deduce that the f2 fragment might originate from a further cleavage of the f1 fragment at a position beyond the residue 701.

To assign the β-DG proteolytic fragments with greater confidence, the MMP-9 digestion of β-DG(654–750) was monitored by RP-HPLC-ESI-MS. A total of 100 μL fractions of the reaction mixture were collected after 0, 1, 2, 3 and 5 hr of incubation and the MMP-9 digestion was stopped adding an equal volume of 0.1% TFA before the RP-HPLC-ESI-MS analysis.

In the RP-HPLC-MS profile registered at time 0, the uncleaved β-DG(654–750) was eluted at 32.66 min (Figs. 3A–3D) with an average mass of β-DG(654–750), corresponding to 10526.8 ± 0.5 amu, as obtained by deconvolution of the ESI mass spectrum (Fig. 3F) registered between 32.58 and 32.97 min (Fig. 3E).

In the RP-HPLC-MS and UV profiles registered after 1 hr of incubation with MMP-9 three additional derivatives eluting at 32.80, 32.20 and 24.90 min were revealed, beside the one corresponding to the uncleaved β-DG(654–750) eluted at 32.66 min (Figs. 4A and 4B). The comparison with the RP-HPLC-MS profiles registered after 5 hr of incubation with MMP-9 (Figs. 4C and 4D) shows that the intensity of the peak corresponding to the derivative eluting at 24.90 min remained constant during the entire incubation time, whereas the intensity of the other peaks decreased. However, the peak of the unreacted β-DG(654–750) could still be detected, at 32.70 min, also after 5 hr of incubation. The deconvolution of the two peaks eluting at 31.78 and 32.12 min allowed to calculate a molecular mass of 10542 ± 0.5 amu for their associated species, about 16 Da higher than the one assigned to the unreacted β-DG(654–750), suggesting the occurrence of two different oxidized forms of β-DG(654–750) (Figs. 4C and 4D). As far as the derivative eluting at 24.90 min is concerned, the average mass obtained by deconvolution (Fig. 4F) of the ESI mass spectrum, registered between 24.60 and 25.05 min (Fig. 4E), corresponded to 3669.5 ± 0.5

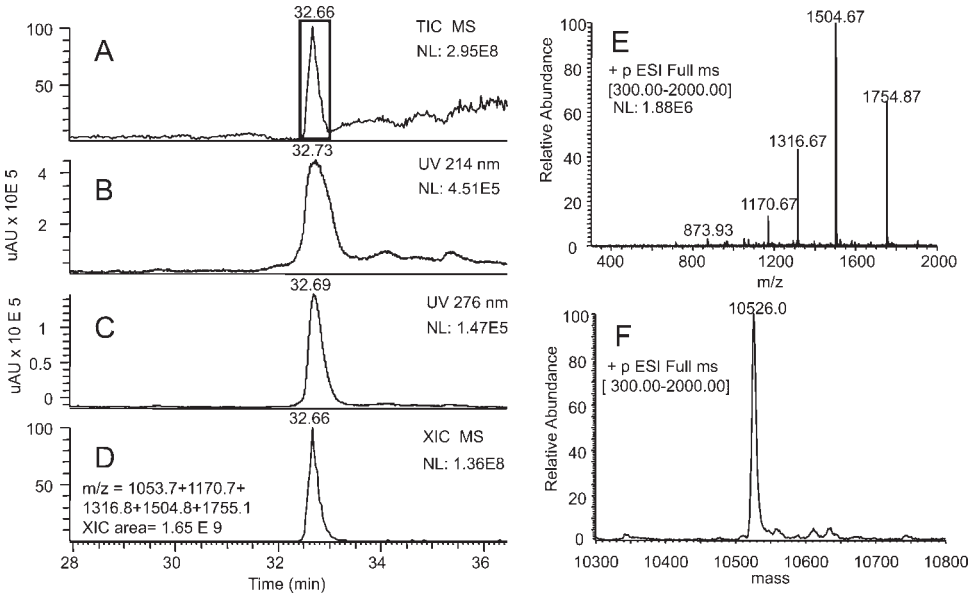

Figure 3. RP-HPLC-ESI-MS profile of β-DG(654–750) registered as TIC (A), UV at 214 nm (B), 276 nm (C), and XIC (D). The ESI spectrum of the species eluting at 32.66 min is reported (E) and the average mass obtained by its deconvolution (F) is 10526.8 $\pm$ 0.5 amu, corresponding to the theoretical mass of β-DG(654–750).

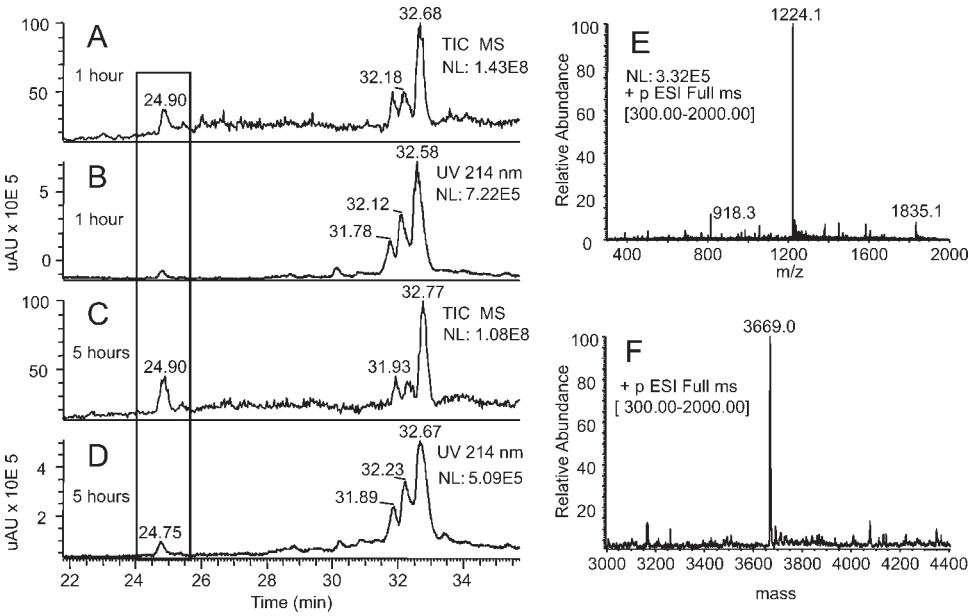

Figure 4. RP-HPLC-ESI-MS profile of β-DG(654–750) after 1 hr of incubation with MMP-9, registered as TIC (A) and UV at 214 nm (B) and after 5 hr of incubation with MMP-9, registered as TIC (C), and UV at 214 nm (D). The ESI spectrum of the species eluting at 24.90 min is reported (E) and the average mass obtained by its deconvolution (F) is 3669.5 $\pm$ 0.5 amu, corresponding to the theoretical mass of the β-DG(654–750) C-terminal fragment, spanning the amino acid positions comprised between 716 and 750.

amu. The application of the XIC analysis allowed to assign the mass value of 3669.5 amu to the β-DG(654–750) C-terminal fragment spanning the amino acid positions 716–750 (Fig. 5C). We expected the XIC analysis to be able to reveal the mass value corresponding to the complementary N-terminal fragment of β-DG(654–750), spanning the amino acid positions 654–715,

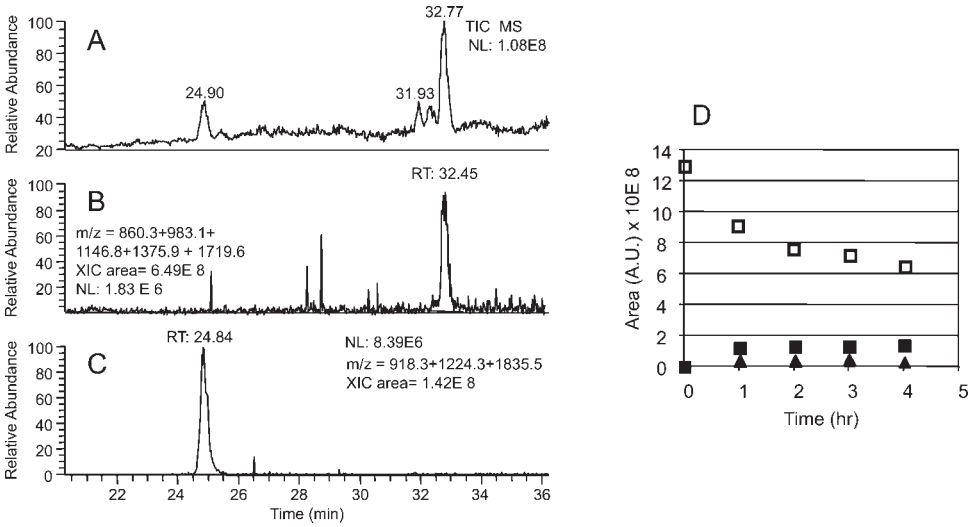

Figure 5. RP-HPLC-ESI-MS profile of β-DG(654–750) after 4 hr of incubation with MMP-9, registered as TIC (A). The Extracted ion current (XIC) analysis application, performed by using 860.3, 983.1, 1146.8, 1375.9, and 1719.6 m/z values for its N-terminal fragment, β-DG(GS-654–715) (B), and 918.3, 1224.3, 1839.5 m/z for its C-terminal fragment β-DG(716–750) (C), is reported. The selected m/z ions are specific of the species investigated (see Materials and Methods). The area of these peaks provides the relative abundances of β-DG(654–750) (□) and of its N-terminal (▲) and C-terminal (■) fragments.

plus the two additional residues GS at the N-terminus. Effectively, the multiple charged ions at 860.3, 983.1, 1146.8, 1375.9 and 1719.6 m/z, corresponding to the 6876.4 amu, which is the theoretical mass value calculated for the fragment GS-β-DG(654–716), were found at 32.45 min (Fig. 5B).

Multiple XIC analysis also allowed measuring the relative abundances of the full-length β-DG(654–750) and of its fragments of 6876.4 and 3669.5 amu during the proteolytic reaction carried out by MMP-9 (Fig. 5). Data show that the relative abundance of β-DG(654–750) decreased, while the relative abundance of its fragments increased, although the N-terminal fragment seemed to be less abundant than the C-terminal fragment for the entire reaction time (Fig. 5D). This would suggest that MMP-9 produced a first cleavage between the amino acid residues His-715 and Leu-716 of β-DG(654–750), generating an N-terminal fragment of 6876.4 amu, which was likely to correspond to the f1 band**,** detected on the Tricine gel in Fig. 1A, and a C-terminal fragment of 3669.5 amu probably corresponding to the f3 band detected on the Tricine gel in Fig. 1B. The N-terminal fragment was probably further processed by MMP-9, which produced a shorter N-terminal fragment (corresponding to the f2 band detected on the gel of Fig. 1A), whereas the C-terminal fragment was quite stable during the entire incubation time.

The RP-HPLC-MS profile registered after 5 hr of incubation of β-DG(654–750) with a nonactivated MMP-9 or with MMP-3 (that was used to activate MMP-9) did not reveal any degradation process, demonstrating the specificity of MMP-9 cleavages (data not shown).

To confirm these assignments, MS/MS fragmentations were carried out on the putative C-terminal fragment of β-DG(654–750), spanning the amino acid positions 716–750 (Fig. 6). The nomenclature for the fragment ions is based on that proposed by Roepstorff and Fohlman (*39*) and modified by Biemann (*40*). The ESI full-scan spectrum showed an abundant triply charged ion at 1224.10 m/z, which was selected as the precursor ion for the MS/MS analysis. The structure confirmation was done by inducing the fragmentation on the triply charged ion at 1224.10 m/z and comparing the observed pattern with the one expected for the specific sequence obtained by the MS-Product (available on the Protein Prospector site). As shown in Fig. 6 the product ion scan of the above triply charged ion exhibited an MS/MS fragmentation spectrum, which confirmed the sequence of this fragment.

DISCUSSION

It is well known from the literature that β-DG is a target for MMP-9, whose enzymatic activity produces a typical 30 kDa β-DG fragment detected both in pathological, as well as in physiological conditions (*9–11*). It was also demonstrated that the 30 kDa fragment lacks the ectodomain, as it can be still detected by a monoclonal antibody directed against the C-terminal cytosolic region of β-DG (*9*). To understand the molecular mechanisms underlying the β-DG cleavage carried out by MMP-9, we have established an *in vitro* system constituted by a recombinant β-DG ectodomain, β-DG(654–750), and a recombinant MMP-9. The MMP-9 digestion of β-DG(654–750) was monitored by two independent techniques: SDS-PAGE coupled to MALDI-TOF MS and RP-HPLC-MS. The experimental data indicate that MMP-9 is able to produce a first proteolytic cleavage between His-715 and Leu-716 of β-DG(654–750), resulting in an N-terminal fragment that is further processed, and a C-ter-

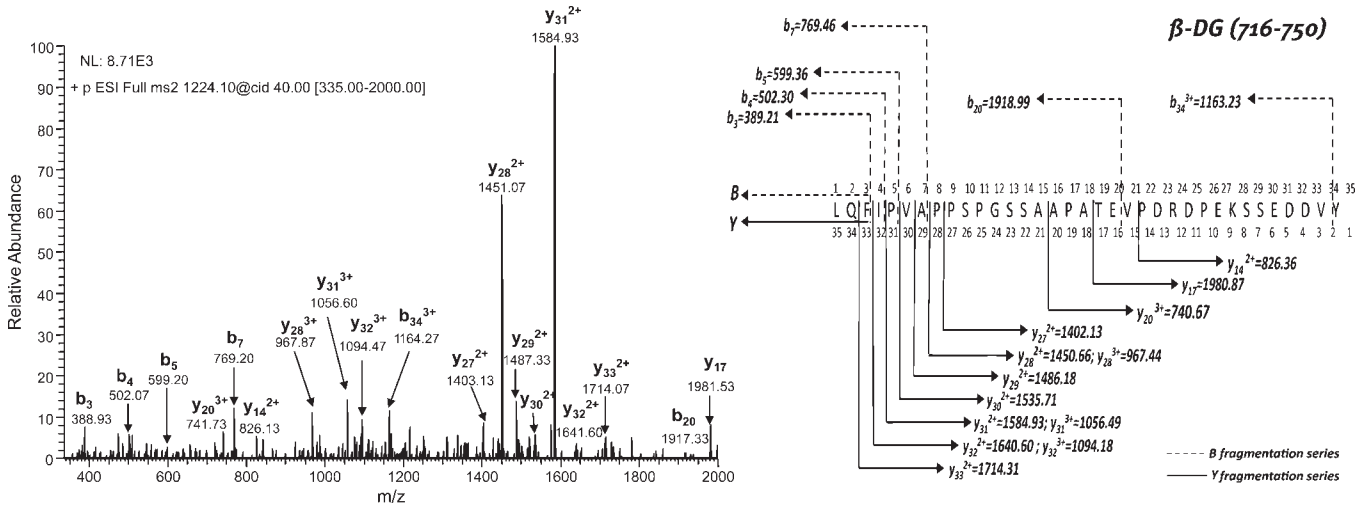

Figure 6. MS/MS experiment performed on the triply charged ion at 1224.10 m/z corresponding to the β-DG(654–750) C-terminal fragment (716–750) originated by the MMP-9 cleavage. The principal fragments of the y and b series are indicated.

minal fragment, which appears to be very stable even after a prolonged incubation with MMP-9 (see Fig. 7).

Although the β-DG(654–750) ectodomain is only a portion of the whole β-DG subunit, MMP-9 interacts very efficiently with it, displaying an affinity (K_m = 1.4(±0.2) × 10^{-4} M), high enough to consider this interaction physiologically relevant. On the other hand, the fairly low enzymatic activity, mostly because of a very slow cleavage rate constant (k_{cat} = 0.09(±0.01) s^{-1}) indicates that the enzyme:substrate complex has to rearrange its conformation to be efficiently processed. This is probably because of the highly flexible and extended conformation of the β-DG ectodomain, which has to be deeply rearranged to reach the transition state, requiring a high activation energy; this suggests that the cleavage event might be regulated by structural changes of the substrate. Interestingly, there is evidence that MMP-2, that is similar to MMP-9, both in structure and substrate recognition, shows an analogous affinity towards β-DG(654–750) (K_m = 4.5(±0.6) × 10^{-4}M) compared with the one displayed by MMP-9, but an higher enzymatic activity (k_{cat}/K_m = 8.5(±1.3) × 10^3 $M^{-1}s^{-1}$, k_{cat} = 3.85(±0.53) s^{-1}).

However, the cleavage produced by MMP-9 is very specific and it results in the appearance of an N-terminal fragment spanning the amino acid positions 654–715 and a C-terminal fragment spanning the positions 716–750. The N-terminal fragment is further processed at its C-term, whereas the C-terminal fragment remains intact for a long time (Fig. 7).

Although consensus sequences for the MMP-9 enzymatic activity have never been identified in target polypeptides, a hydrophobic amino acid was detected most often as the P1' residue (*41*). Interestingly, MMP-9 produces ten specific cleavages on the insulin chains: one out of ten cleavage sites displays the sequence His-Leu and leucine was found as the P1' residue in six out of ten cleavage sites (*42*).

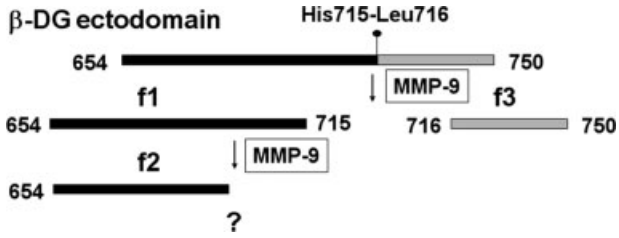

Figure 7. Proposed scheme of the β-DG(654–750) proteolytic cleavage induced by MMP-9. MMP-9 is able to produce a first proteolytic cleavage between His-715 and Leu-716 of β-DG(654–750), resulting in an N-terminal fragment (f1), that is further reduced to a shorter N-terminal fragment (f2), and a C-terminal fragment (f3) that is very stable.

Recombinant β-DG(654–750) belongs to the class of the natively unfolded proteins, as it is able to specifically bind its biological partner, α-DG, although it lacks a well defined three-dimensional structure (*37, 38*). An NMR analysis showed that β-DG(654–750) displays an N-terminal region, characterized by a restricted mobility and by the presence of the binding epitope for α-DG, and a highly flexible C-terminal portion of about 30 amino acids. Furthermore, the N-terminal region was shown to interact with an anionic detergent, such as sodium dodecyl-sulphate (SDS), whereas the C-terminal portion remained largely unaffected even at a very high SDS concentration (*43*). It is noteworthy that the β-DG linear sequence comprised between the amino acid positions 691 and 719 contains the α-DG binding epitope (*38*). Therefore, the specific cleavage produced by MMP-9 at the amino acid positions 715–716, overlapping with the end of the α-DG binding epitope, removes the α-DG binding epitope impairing the α-DG/β-DG interface. This might explain the presence of the 30 kDa β-DG fragment, which con-

tains the entire cytosolic domain, produced by MMP-9 in healthy tissues, such as peripheral nerve, bladder, lung, kidney (*10*) and in normal human keratinocytes (*11*). Indeed, the β-DG ectodomain shedding produced by MMP-9 removes the α-DG binding epitope interrupting the link between the extracellular matrix and the cytoskeleton. Since it has been proposed that the interaction between α-DG and β-DG may trigger a signal transduction across the cell membrane (*44, 45*), MMP-9 could modulate the signalling through the proteolytic removal of the α-DG binding epitope within the β-DG ectodomain. However, its fairly low enzymatic efficiency under our conditions might indicate that this event is finely modulated by conformational changes of β-DG. The recent discovery of a β-DG processing carried out by MMP-9 in response to enhanced neuronal activity (*23, 24*) would strengthen the hypothesis that MMP-9 cooperates with the DG complex in the signal transduction.

ACKNOWLEDGEMENTS

This work was supported by Telethon-Italy (grant no. GGP06225) and the Italian Space Agency (ASI 2005 OSMA). The authors thank Prof. Ghislain Opdenakker and Dr. Philippe Van den Steen for the generous gift of recombinant MMP-9, Dr. Maria Giulia Bigotti for critical reading of the manuscript, and Salvatore Meo for his technical help with the illustrations.

REFERENCES

1. Ibraghimov-Beskrovnaya, O., Ervasti J. M., Leveille, C. J., Slaughter, C. A., Sernett, S. W., and Campbell, K. P. (1992) Primary structure of dystrophin-associated glycoproteins linking dystrophin to the extracellular matrix. *Nature* **355**, 696–702.
2. Henry, M. D. and Campbell, K. P. (1999) Dystroglycan inside and out. *Curr. Opin. Cell Biol.* **11**, 602–607.
3. Cartaud, A., Coutant, S., Petrucci, T. C., and Cartaud, J. (1998) Evidence for in situ and in vitro association between β-dystroglycan and the subsynaptic 43K rapsyn protein. Consequence for acetylcholine receptor clustering at the synapse. *J. Biol. Chem.* **273**, 11321–11326.
4. Jung, D., Yang, B., Meyer, J., Chamberlain, J. S., and Campbell, K. P. (1995) Identification and characterization of the dystrophin anchoring site on β-dystroglycan. *J. Biol. Chem.* **270**, 27305–27310.
5. Yang, B., Jung, D., Motto, D., Meyer, J., Koretzky, G., and Campbell, K. P. (1995) SH3 domain-mediated interaction of dystroglycan and Grb2. *J. Biol. Chem.* **270**, 11711–11714.
6. Di Stasio, E., Sciandra, F., Maras, B., Di Tommaso, F., Petrucci, T.C., Giardina, B., and Brancaccio, A. (1999) Structural and functional analysis of the N-terminal extracellular region of β-dystroglycan. *Biochem. Biophys. Res. Commun.* **266**, 274–278.
7. Barresi, R. and Campbell, K. P. (2006) Dystroglycan: from biosynthesis to pathogenesis of human disease. *J. Cell. Sci.* **119**, 199–207.
8. Muntoni, F., Torelli, S., and Brockington, M. (2008) Muscular dystrophies due to glycosylation defects. *Neurotherapeutics* **5**, 6278–632.
9. Losasso, C., Di Tommaso F., Sgambato, A., Ardito, R., Cittadini, A., Giardina, B., Petrucci, T. C., and Brancaccio, A. (2000) Anomalous dystroglycan in carcinoma cell lines. *FEBS Lett.* **484**, 194–198.
10. Yamada, H., Saito, F., Fukuta-Ohi, H., Zhong, D., Hase, A., Arai, K., Okuyama, A., Maekawa, R., Shimizu, T., and Matsumura, K. (2001) Processing of β-dystroglycan by matrix metalloproteinase disrupts the link between the extracellular matrix and cell membrane via the dystroglycan complex. *Hum. Mol. Genet.* **10**, 1563–1569.
11. Herzog, C., Has, C., Franzke, C. W., Echtermeyer, F.G., Schlötzer-Schrehardt, U., Kröger, S., Gustafsson, E., Fässler R., and Bruckner-Tuderman, L. (2004) Dystroglycan in skin and cutaneous cells: β-subunit is shed from the cell surface, *J. Invest. Dermatol.* **122**, 1372–1380.
12. Matsumura, K., Zhong, D., Saito, F., Arai, K., Adachi, K., Kawai, H., Higuchi, I., Nishino, I., and Shimizu, T. (2005) Proteolysis of β-dystroglycan in muscular diseases. *Neuromuscul. Disord.* **15**, 336–341.
13. Milner, R., Hung, S., Wang, X., Spatz, M., and del Zoppo, G. J. (2008) The rapid decrease in astrocyte-associated dystroglycan expression by focal cerebral ischemia is protease-dependent. *J. Cereb. Blood Flow Metab.* **28**, 812–823.
14. Armstrong, S. C., Latham, C. A., and Ganote C. E. (2003) An ischemic β-dystroglycan (betaDG) degradation product: correlation with irreversible injury in adult rabbit cardiomyocytes. *Mol. Cell Biochem.* **242**, 71–79.
15. Wimsey, S., Lien, C. F., Sharma, S., Brennan, P. A., Roach, H. I., Harper, G. D, and Córecki, D. C. (2006) Changes in immunolocalisation of β-dystroglycan and specific degradative enzymes in the osteoarthritic synovium. *Osteoarthritis Cartilage* **14**, 1181–1188.
16. Jing, J., Lien, C. F., Sharma, S., Rice, J., Brennan, P. A., and Córecki, G. C. (2004) Aberrant expression, processing and degradation of dystroglycan in squamous cell carcinomas. *Eur. J. Cancer* **40**, 2143–2151.
17. Zhong, D., Saito, F., Saito, Y., Nakamura, A., Shimizu, T., and Matsumura, K. (2006) Characterization of the protease activity that cleaves the extracellular domain of β-dystroglycan. *Biochem. Biophys. Res. Commun.* **345**, 867–871.
18. Agrawal, S., Anderson, P., Durbeej, M., van Rooijen, N., Ivars, F., Opdenakker, G., and Sorokin, L. M. (2006) Dystroglycan is selectively cleaved at the parenchymal basement membrane at sites of leukocyte extravasation in experimental autoimmune encephalomyelitis. *J. Exp. Med.* **203**, 1007–1019.
19. Morgunova, E., Tuuttila, A., Bergmann, U., Isupov, M., Lindqvist, Y., Schneider, G., and Tryggvason, K. (1999) Structure of human pro-matrix metalloproteinase-2: activation mechanism revealed. *Science* **284,** 1667–1670.
20. Aureli, L., Gioia, M., Cerbara, I., Monaco, S., Fasciglione, G. F., Marini, S., Ascenzi, P., Topai, A., and Coletta, M. (2008) Structural bases for substrate and inhibitor recognition by matrix metalloproteinases. *Curr. Med. Chem.* **15**, 2192–2222.
21. Monaco, S., Sparano, V., Gioia, M., Sbardella, D., Di Pierro, D., Marini, S., and Coletta, M. (2006) Enzymatic processing of collagen IV by MMP-2 (gelatinase A) affects neutrophil migration and it is modulated by extracatalytic domains. *Protein Sci.* **15**, 2805–2815.
22. Gioia, M., Monaco, S., Van Den Steen, P. E., Sbardella, D., Grasso, G., Marini, S., Overall, C. M., Opdenakker, G., and Coletta, M. (2009) The collagen binding domain of gelatinase A modulates degradation of collagen IV by gelatinase B. *J. Mol. Biol.* **386**, 419–434.
23. Kaczmarek, L., Lapinska-Dzwonek, J., and Szymczak, S. (2002) Matrix metalloproteinases in the adult brain physiology: a link between c-Fos, AP-1 and remodeling of neuronal connections? *EMBO J.* **21**, 6643–6648.
24. Michaluk, P., Kolodziej, L., Mioduszewska, B., Wilczynski, G. M, Dzwonek, J., Jaworski, J., Gorecki, D. C, Ottersen, O. P, and Kaczmarek, L. (2007) β-dystroglycan as a target for MMP-9, in response to enhanced neuronal activity. *J. Biol. Chem.* **282**, 16036–16041.
25. Bozzi, M., Morlacchi, S., Bigotti, M. G., Sciandra, F., and Brancaccio, A. (2009) Functional diversity of dystroglycan. *Matrix Biol.* **78**, 179–187.

26. Kammerer, R. A., Schulthess, T., Landwehr, R., Lustig, A., Fischer, D., and Engel, J. (1998) Tenascin-C hexabrachion assembly is a sequential two-step process initiated by coiled-coil α-helices. *J. Biol. Chem.* **273**, 10602–10608.
27. Van den Steen, P. E., Van Aelst, I., Hvidberg, V., Piccard, H., Fiten, P., Jacobsen, C., Moestrup, S. K., Fry, S., Royle, L., Wormald, M. R,Wallis, R., Rudd, P. M., Dwek, R. A., and Opdenakker, G. (2006) The hemopexin and O-glycosylated domains tune gelatinase B/MMP-9 bioavailability via inhibition and binding to cargo receptors. *J. Biol. Chem.* **281**, 18626–18637.
28. Masure, S., Proost, P., Van Damme, J., and Opdenakker, G. (1991) Purification and identification of 91-kDa neutrophil gelatinase. Release by the activating peptide interleukin-8. *Eur. J. Biochem.* **198**, 391–398.
29. Nordhoff, E., Schurenberg, M., Thiele, G., Lubbert, C., Kloeppel, K. D., Theiss, D., Lehrach, H., and Gobom, J. (2003) Sample preparation protocols for MALDI-MS of peptides and oligonucleotides using prestructured sample supports. *Int. J. Mass Spectrom.* **226**, 163–180.
30. Wilkins, M. R., Lindskog, I., Gasteiger, E., Bairoch, A., Sanchez, J. C., Hochstrasser, D. F., and Appel, R. D. (1997) Detailed peptide characterization using PEPTIDEMASS—a World-Wide-Web-accessible tool. *Electrophoresis* **18**, 403–408.
31. Wilkins, M. R., Gasteiger, E., Bairoch, A., Sanchez, J. C., Williams, K. L., Appel, R. D., and Hochstrasser, D. F. (1999) Protein identification and analysis tools in the ExPASy server. *Methods Mol. Biol.* **112**, 531–552.
32. Zhang, Z. and Marshall, A. G. (1998) A universal algorithm for fast and automated charge state deconvolution of electrospray mass-to-charge ratio spectra. *J. Am. Soc. Mass Spectrom.* **9**, 225–233.
33. Ong, S. E. and Mann, M. (2005) Mass spectrometry-based proteomics turns quantitative. *Nat. Chem. Biol.* **1**, 252–262.
34. Steen, H., Jebanathirajah, J. A., Rush, J., Morrice, N., and Kirschner, M. W. (2006) Phosphorylation analysis by mass spectrometry: myths, facts, and the consequences for qualitative and quantitative measurements. *Mol. Cell. Proteomics* **5**, 172–181.
35. Uversky, V. N. (2002) Natively unfolded proteins: a point where biology waits for physics. *Protein Sci.* **11**, 739–756.
36. Tompa, P. (2002) Intrinsically unstructured proteins. *Trends Biochem. Sci.* **27**, 527–533.
37. Boffi, A., Bozzi, M., Sciandra, F., Woellner, C., Bigotti, M. G,Ilari, A., and Brancaccio, A. (2001) Plasticity of secondary structure in the N-terminal region of β-dystroglycan. *Biochim. Biophys. Acta* **1546**, 114–121.
38. Bozzi, M., Bianchi, M., Sciandra, F., Paci, M., Giardina, B., Brancaccio, A., and Cicero, D. O. (2003) Structural characterization by NMR of the natively unfolded extracellular domain of β-dystroglycan: toward the identification of the binding epitope for α-dystroglycan. *Biochemistry* **42**, 13717–13724.
39. Roepstorff, P. and Fohlman, J. (1984) Proposal for a common nomenclature for sequence ions in mass spectra of peptides. *Biomed. Mass Spectrom.* **11**, 601.
40. Bieman, K. (1989) Tandem mass spectrometry applied to protein structure problems. *Biochem. Soc. Trans.* **17**, 237–243.
41. Van den Steen, P. E., Proost, P., Grillet, B., Brand, D. D., Kang, A. H., Van Damme, J., and Opdenakker, G. (2002) Cleavage of denatured natural collagen type II by neutrophil gelatinase B reveals enzyme specificity, post-translational modifications in the substrate, and the formation of remnant epitopes in rheumatoid arthritis. *FASEB J.* **16**, 379–389.
42. Descamps, F. J, P.E.Van den Steen,Martens, E., Ballaux, F., Geboes, K., and Opdenakker, G. (2003) Gelatinase B is diabetogenic in acute and chronic pancreatitis by cleaving insulin, *FASEB J.* **17**, 887–889.
43. Bozzi, M., Di Stasio, E., Cicero, D. O., Giardina, B., Paci, M., and Brancaccio, A. (2004) The effect of an ionic detergent on the natively unfolded β-dystroglycan ectodomain and on its interaction with α-dystroglycan. *Protein Sci.* **13**, 2437–2445.
44. Sotgia, F., Lee, H., Bedford, M. T., Petrucci, T. C., Sudol, M., and Lisanti M. P. (2001) Tyrosine phosphorylation of β-dystroglycan at its WW domain binding motif, PPxY, recruits SH2 domain containing proteins. *Biochemistry* **40**, 14585–14592.
45. Zhou, Y. W., Thomason, D. B., Gullberg, D., and Jarrett, H. W (2006) Binding of laminin α1-chain LG4-5 domain to α-dystroglycan causes tyrosine phosphorylation of syntrophin to initiate Rac1 signaling. *Biochemistry* **45**, 2042–2052.